Water-Leaching Rates of Halides from Polymers

NAVA NARKIS,* MOSHE NARKIS,* and ITZCHAK BERKOVITZ,
Departments of Environmental and Water Resources Engineering and Chemical Engineering, Technion-City, Haifa 32000, Israel

Synopsis

Water-leaching experiments of halides from polymers were carried out in batch and continuous systems. The effects of flow rate, temperature, and salt content on the leaching kinetics were investigated. Different thermoplastic polymers were used as the salt carrier, and the release kinetics from them was established. NaCl, NaBr, and NaI were leached out completely from nylons, while NaF could only be partially removed. Release mechanisms involving diffusion, capillary flow, and fracturing were described based upon the leaching kinetics and porosity distribution in the resulting foams.

INTRODUCTION

Water-soluble compounds dispersed in polymers can be leached out by contact with water. Fossey[1] produced polyethylene foams and Gregorian[2] prepared crosslinked microporous polyolefin films. Porous high-density polyethylene films were produced by Bigg.[3] Polyurethane foams were prepared by Smith.[4] Thomas[5] described the leaching method as suitable for preparation of flexible foams. Rigid amorphous polymeric foams were reported by Nielsen and Lee,[6] Narkis and Joseph,[7,8] Narkis et al.,[9] and Glas.[10] All these authors have employed the water-leaching method and all have reported that essentially open-cell structures have been obtained.

Whereas fast leaching of the temporary filler is desired for production of open-cell structures, water chemists are interested in slow and controlled leaching rates for dosing purposes of active chemicals into the contacting water.[11] Thus it is important to determine and analyze leaching rates over a wide range of conditions (temperatures, components and concentrations) to cover the needs of potential open-cell foam producers as well as of water chemists interested in employing the leaching idea for their purposes. Preliminary leaching rate data from granules (2–3 mm) covering time periods up to two months were reported by Narkis and Narkis.[12] Short leaching periods, up to 100 min, were studied by Bigg[3] for production of 500 μm thick HDPE films (dispersed NaCl particle sizes of 20–200 μm).

* On sabbatical leave at the University of Connecticut, Civil Engineering, Chemical Engineering and Institute of Materials Science, Storrs, CT 06268.

Journal of Applied Polymer Science, Vol. 27, 1795–1807 (1982)
 CCC 0021-8995/82/051795-13$02.30

The objective of the present work is to show how the leaching rate varies as a function of temperature and salt concentration for different polymer–halide systems.

EXPERIMENTAL

A summary of the polymers used in the present work is given in Table I. Commercial halides in the size range of 40–200 μm were used as received. Granules (2–3 mm) of polymer–halide were prepared by mixing on a heated two-roll mill and grinding for small batch leaching experiments, and by extrusion and granulation for continuous leaching experiments. A batch system consisted of a 2000-mL beaker containing 10 g polymer–halide particles, 1000 mL water, and a magnetic stirrer. A continuous system consisted of a 2.3 cm i.d. glass tube (tube and shell type) 60 cm long packed with 200 g polymer–salt particles. Distilled water was pumped into the packed tube at a constant rate (300–1500 mL/h) from a constant temperature bath. Water maintained at the same temperature was pumped from a separate reservoir through the annulus to keep the column at a constant temperature. Halide concentration in the leaching water was measured with a Methron conductivity instrument using various types of electrodes, including a very sensitive electrode for dilute solutions (about 0.1 mg/L).

Salt content in the polymer–halide granules before and sometimes after contact with water was determined by drying at 105°C and combustion at 600°C.

Porosity measurements were done by using an Aminco mercury porosimeter with mercury pressures up to 15,000 psi. Integral and differential porosity–pressure (or size) curves were obtained.

TABLE I
List of Polymers and Properties[a] at Room Temperature

Polymers	Manufacturer grade	Density g/mL	Water absorption (% w/w 24 h)	Tensile strength (psi)	Tensile elongation (%)
Polystyrene, PS	IPE, HF-55	1.05	0.05	5,300–7,900	1–2
Polysulfone, PSF	Union Carbide P-1700	1.24	0.22	15,400[b]	50–100
Polycarbonate, PC	GE, Lexan 101	1.20	0.15	9,500	110
Styrene–acrylonitrile, SAN	Montedison, Kostil	1.08	0.25	9,000–12,000	1–4
Nylon 6	Dupont, Zytel	1.13	1.6	10,000[c]	300[c]
Nylon 11	Emzer	1.04	0.3	8,000	300
Poly(methyl methacrylate), PMMA	ICI MH-253	1.19	0.3	8,000–11,000	2–7

[a] J. Brandrup and E. H. Immergut, Eds., *Polymer Handbook*, Interscience, New York, 1966; *Modern Plastics Encyclopedia*, Interscience, New York, 1981.

[b] Flexural strength.

[c] In equilibrium with 50% RH.

RESULTS AND DISCUSSION

Previous strength studies[7-9] have shown that PMMA foams produced by NaCl leaching had low and similar strength values for void contents from 5 to 45% by volume. This significant strength reduction already caused by "adding" 5% voids to the structure, coupled with the fact that open-cell structures have been reported by all the researchers, has led to the interpretation of the structure as totally cracked. Such a cracked structure is formed during the long extraction period by large internal forces related to high osmotic pressures developed in the closed cells containing the salt particles. Eventually the high pressure will burst the thin walls of the enclosing polymer. The magnitude of these osmotic pressures depends on the molar saturation concentration of the halide–water solution in the closed cell. Thus, the saturation solubility of the salt affects the leaching mechanism by determination of the internal osmotic pressures and not by the salt concentration difference between the saturation concentration and the salt concentration in the contacting water. This leaching mechanism is entirely different from the water-leaching mechanism of water-soluble polymers from other polymers. In the latter case, because of the high molecular weight of the extractable polymer, very low osmotic pressures can be developed and therefore the process is diffusion controlled. The structure of porous polymers from which water-soluble polymers have been leached out is thus unfractured by osmotic pressures. The porous structure resembles the original distribution of the dispersed leachable polymer in the continuous polymer.

The leaching mechanism in halide–polymer systems leading to fractured structures will thus depend upon the halide type and concentration, and upon temperature. In systems characterized by insignificant physical or chemical interactions between the salt and polymer, the halide type dictates the water saturation solubility and the upper limit of the osmotic pressure. The concentration of the halide determines the thickness of the wall around the salt particle. Obviously, higher concentrations will lead to thinner walls easing the fracturing process as well as enhancing the water diffusion into the closed cells. The temperature effects can be discussed from at least three aspects: a temperature increase will enhance the leaching rate by (a) increasing the water diffusion rate into the closed cell through its encompassing walls, (b) increasing the internal osmotic pressure (via the saturation molar concentration and the temperature itself), and (c) easing the fracturing process owing to the decreasing mechanical strength of the polymeric cell walls.

Some physical properties of sodium halides used in the present work are summarized in Table II. NaF and NaCl were studied in mixtures with all the polymers listed in Table I, whereas NaBr and NaI were studied in mixtures with nylon 6 and nylon 11 only. The molar saturation solubilities of NaCl and NaF differ by a factor of 6, as shown in Table II. Thus significantly higher internal osmotic pressures are expected in NaCl mixtures compared with NaF mixtures. The salt density is also important, and if comparisons are made for an equal weight concentration, it is clear that the denser salt particles will be surrounded by thicker polymer walls which will slow the water diffusion rate and delay the fracturing process because of strengthening of the walls. Another parameter that determines the walls thickness is the particle size. Smaller particle sizes result in thinner walls. It is thus clear that numerous parameters affect the leaching process, making the mechanism rather complicated. It is also important

TABLE II
Physical Properties of Halides[a]

Halide	M (g/mol)	Density (g/mL)	mp (°C)	Solubility in water[b] Cold (g/100 mL)	Hot (g/100 mL)	Cold (mol/L)	Hot (mol/L)
NaF	42	2.56^{41}	993	4.2^{10}	$4.9^{93.3}$	0.10	0.12
NaCl	58.4	2.16^{25}	801	35.7^{0}	39.1^{100}	0.61	0.67
NaBr	102.9	3.20^{25}	747	116^{50}	121^{100}	1.13	1.18
NaI	149.9	3.67^{25}	661	184^{25}	302^{100}	1.23	2.01

[a] Kirk-Othmer Encyclopedia of Chemical Technology, 3rd ed., Vol. 10, Wiley, New York 1980. R. C. Weast, *Handbook of Chemistry and Physics*, CRC Press, Cleveland, Ohio, 1975–76.
[b] Superior figures designate temperature in degrees centigrade.

to point out that "fresh" surfaces (formed by grinding) respond to leaching with water differently than "original" surfaces (surfaes that were in contact with a mold or die surfaces). Original surfaces seem to consist of thin polymer-rich skins delaying *the leaching process* initially. Finally, the sizes of the granules are also important since they determine the contact surface between the water and the particles.

The effect of water flow rate through a packed column with NaCl–PS granules is shown in Figure 1. Higher flow rates of water result in lower salt concentration in the discharged water. By careful analysis, however, it is found that the dominant factor affecting the leaching kinetics is the contact time and not the flow rate; thus at a given time $t = t_1$ the rate of salt leaching from the polymer is given by

$$-\frac{d(\text{salt})}{dt} = C_i Q_i = \text{constant} \tag{1}$$

where Q_i are different flow rates and C_i are the corresponding salt concentrations in the discharged water at time $t = t_1$. Verification of eq. (1) is shown in Figure 2 where CQ values are plotted against time for the three flow rates given in Figure

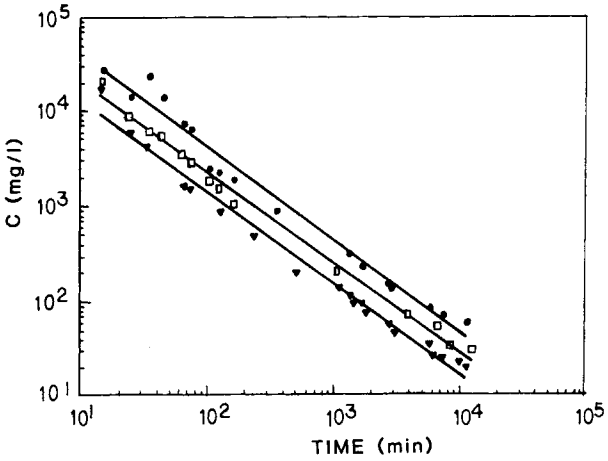

Fig. 1. Effect of water flow rate on concentration–time relationships in continuous leaching experiments of NaCl from 20 phr NaCl–PS granules at 40°C. Flow rates: (●) 500, (□) 1000, (▼) 1500 mL/h.

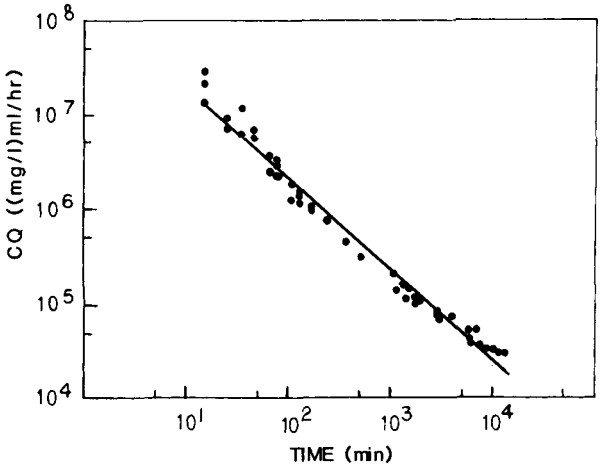

Fig. 2. Replotting of Fig. 1 data as CQ vs. time.

1 (i = 1, 2, 3). Figures 1 and 2 show that in the experimental ranges studied, power law equations can be fitted to the data. The percent salt removed from the granules can be calculated from the previous data by a summation procedure, and the resulting curve is shown in Figure 3. In the conditions described, salt-free granules are obtained after about one week.

Similar results were found in continuous leaching experiments studying NaF–PS granules (see Fig. 4). The temperature effect was investigated by using 20 phr (parts per hundred) NaF–PS granules and the following empirical equation fitted to the data:

$$CQ = 10^{7.69}t^{-1.14} \qquad T = 25°C \tag{2}$$

$$CQ = 10^{7.75}t^{-1.15} \qquad T = 40°C \tag{3}$$

$$CQ = 10^{7.85}t^{-1.17} \qquad T = 70°C \tag{4}$$

where C is the NaF concentration (mg/L) in the discharging water, Q is the water

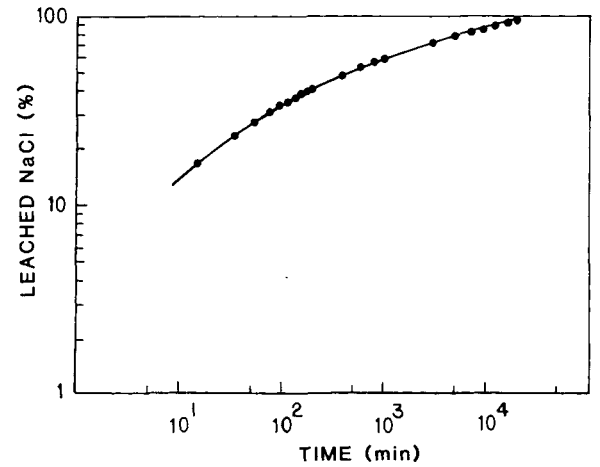

Fig. 3. Progress of NaCl leaching from NaCl–PS granules at 40°C. Based on Fig. 1 data.

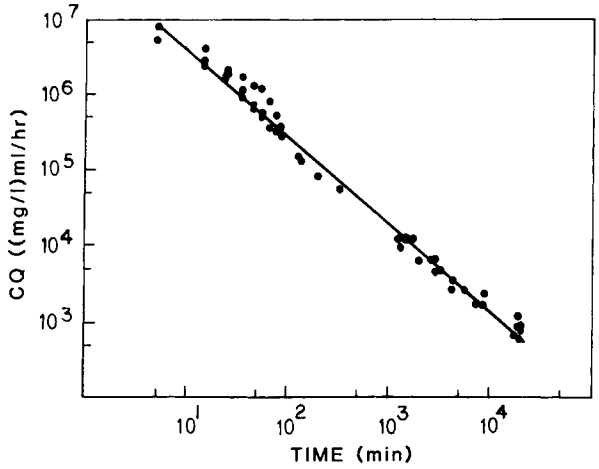

Fig. 4. Correlation of CQ vs. time in continuous leaching experiments of NaF from 20 phr NaF–PS granules at 40°C.

flow rate (mL/h), and t is the time (min). These empirical equations were further integrated to yield the percent of NaF removed with time for three temperatures, as shown in Figure 5. Two important conclusions can be drawn from this figure: (1) the temperature effect is small, and (2) less than 15% NaF have been leached out during one week at 70°C (NaCl leaches out completely under similar conditions). The small temperature effect is related to the small variation of NaF solubility with temperature (Table II). The relatively small percent of NaF removal is attributed to its low water solubility (see Table II) and consequently low osmotic pressures. The fracturing salt release mechanism in NaF–PS granules is thus limited to thin layers enclosing the granules, and the bulk of the granules remain intact.

The effect of salt concentration S (phr) in the polymer on the leaching rate was studied in continuous experiments using 10, 20, and 30 phr NaF–PS granules. The independency of C/S (mg/L/phr) values upon S was reported in a previous

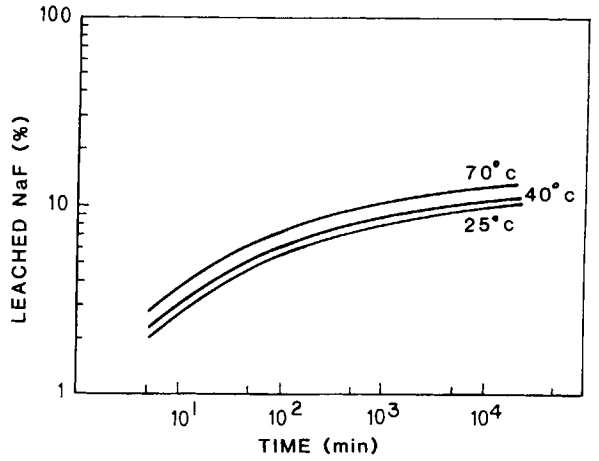

Fig. 5. Progress of NaF leaching from 20 phr NaF–PS granules at three temperatures in continuous experiments.

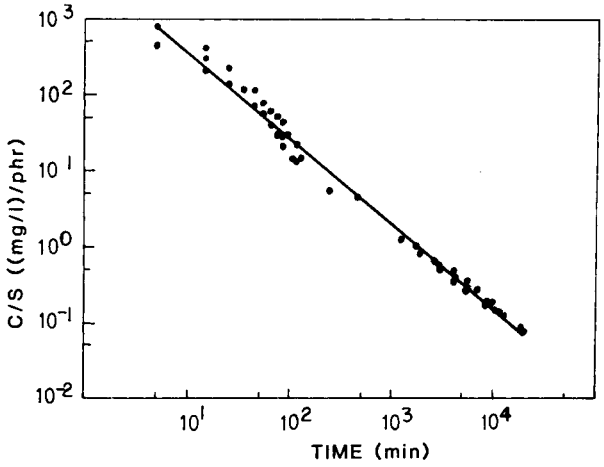

Fig. 6. Dependence of C/S on time in continuous leaching experiments of NaF from NaF–PS granules at 40°C. Compounds contained NaF concentrations of S = 10, 20, and 30 phr.

publication for NaCl–PS compounds[11] and verified here for NaF/PS compounds, as shown in Figure 6.

In a previous publication[11] the leaching kinetics of NaCl from polystyrene, thermosetting polyester, crosslinked polyethylene, and high-density polyethylene was studied. Polystyrene showed the highest salt release rate followed by polyester, XLPE, and HDPE. In the present work, polystyrene was compared to other amorphous thermoplastic resins, as shown in Figures 7 and 8. At 40°C and after 10 min, PS releases only about 15% of its salt while SAN, PC, and PSF have already released 45–55% of their salt contents. After one week PS has released all its salt, whereas SAN still has 15% of its unreleased salt and PC and PSF have 30% unleached NaCl. The exact reasons for the exceptional behavior of PS as shown in Figure 7 are not known.

The leaching experiments at 100°C as shown in Figure 8 exhibit different behavior (compared to 40°C) for PS and SAN where the leaching kinetics is

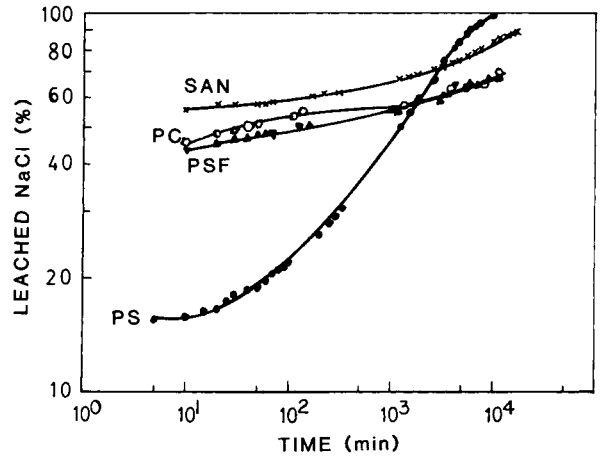

Fig. 7. Progress of NaCl leaching from different polymers in batch experiments at 40°C.

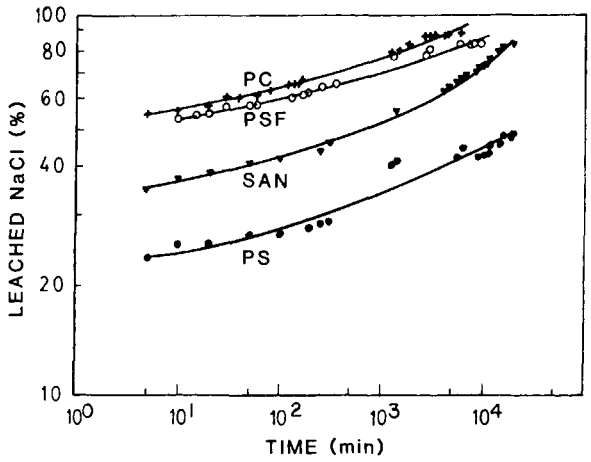

Fig. 8. Progress of NaCl leaching from different polymers in batch experiments at 100°C.

apparently delayed. This result is actually an artifact since under such experimental conditions the PS or SAN particles tend to agglomerate and coalesce, thereby decreasing gradually their contact surface with water during the leaching experiments. The 100°C temperature is well below the glass transition temperatures of PC and PSF; therefore, these polymers behave normally, showing higher leaching rates at the higher temperature.

Nylon–halide–water systems are an intriguing topic for leaching studies. Nylon–halide systems[13,14] and nylon–water systems[15] have been the subject of numerous investigations. The interaction between salts and polar nylon is well known to affect appreciably the polymer physical and mechanical properties. In fact, to produce nylon–halide samples one can immerse nylon films, or powders, in saturated salt solutions, and within a few hours a significant concentration of the salt is found in the polymer.[14] The exact degree of binding, or even formation of a coordination complex,[16] depends on the specific nylon and halide used. In the present work, nylon 6 and nylon 11 were studied where nylon 6, the

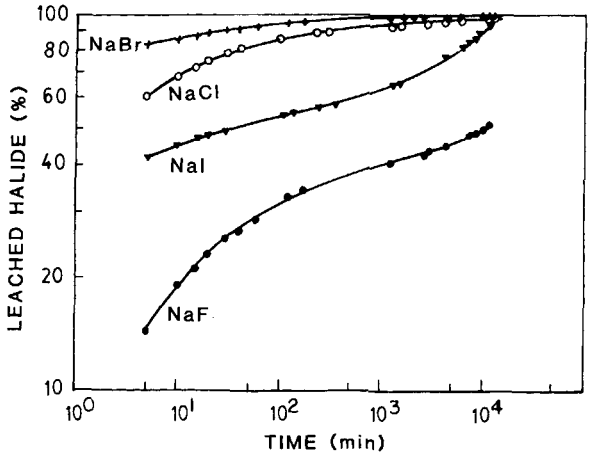

Fig. 9. Progress of halides leaching from nylon 11 in batch experiments at 40°C.

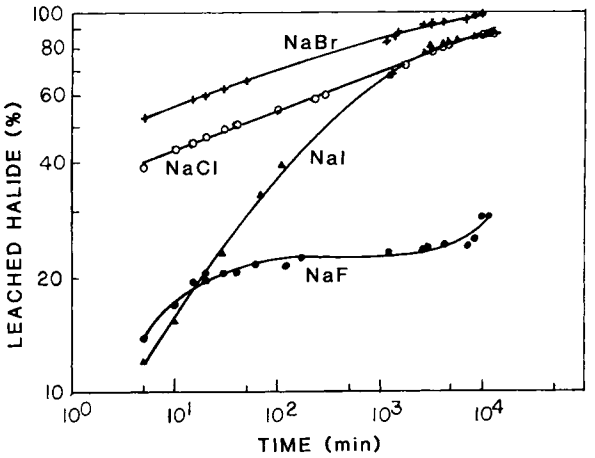

Fig. 10. Progress of halides leaching from nylon 6 in batch experiments at 40°C.

more polar one, absorbs more water and is expected to yield higher binding degrees with halides. The halides investigated can be classified according to their electronegativity, where the highest electronegative compound, NaF, is expected to give the strongest binding to the polar nylon chains. Diffusion of water and ions in polar nylon increases the importance of diffusion mechanisms and consequently decreases the importance of fracturing mechanisms during the salt leaching process. The nylon–halide–water systems seem to be more complicated for analysis than the previous thermoplastic–halide systems where the halide behaves like an inert filler and water has a small effect on the polymer properties. The nylon–halide–water systems represent cases where nylon–nylon, nylon–halide, and nylon–water interactions are important, affecting the polymer properties and the leaching process.

The water-leaching kinetics of halides from nylon 11 and nylon 6 at 40°C are shown in Figures 9 and 10. Comparison of these figures shows that the more

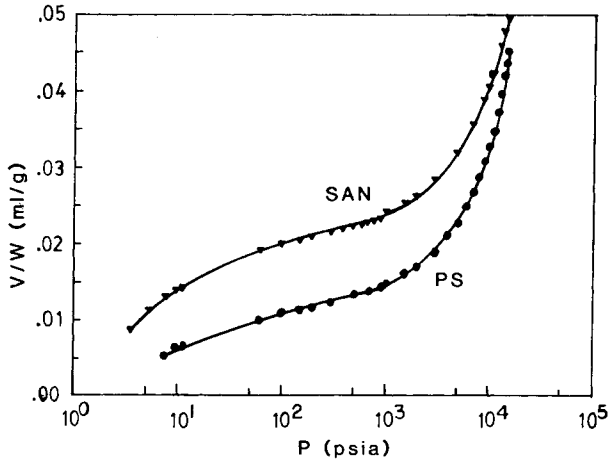

Fig. 11. Integral porosity–pressure curves: (●) PS foam produced by leaching 11.0 phr NaCl; (▼) SAN foam produced by leaching 7.7 phr NaCl; (V) Hg volume; (W) sample weight.

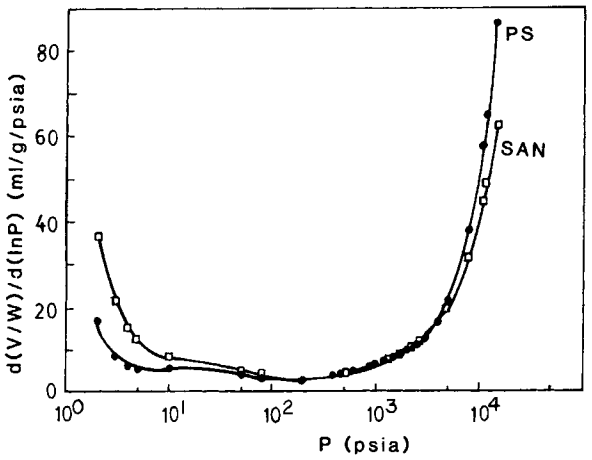

Fig. 12. Differential porosity curves derived from Fig. 11.

polar polymer, nylon 6, which has a better water absorption, gives slower leaching rates probably because of greater binding of the salt to its polar groups. The two nylons are shown to bind better the more electronegative halides, resulting in slower leaching kinetics, with the exception of NaI. This exceptional behavior of NaI is presently not understood. Here again it is shown that during one week almost complete removal of NaCl, NaBr, and NaI has been achieved while only 30% and 50% of NaF have been leached out from nylon 6 and nylon 11, respectively. These results agree with the previous conclusion regarding the incomplete removal of NaF from PS (15% during one week) because of the too-low osmotic pressures developed. The higher values found for nylons are attributed to increasing the importance of diffusion processes of water molecules and ions.

Detailed porosity measurements may shed some additional light on the leaching mechanisms involved by providing porosity–size distribution curves. By increasing the pressure on the penetrating mercury, smaller and smaller pores "show up" and their sizes estimated from the pressure by $D = 175/P$, where

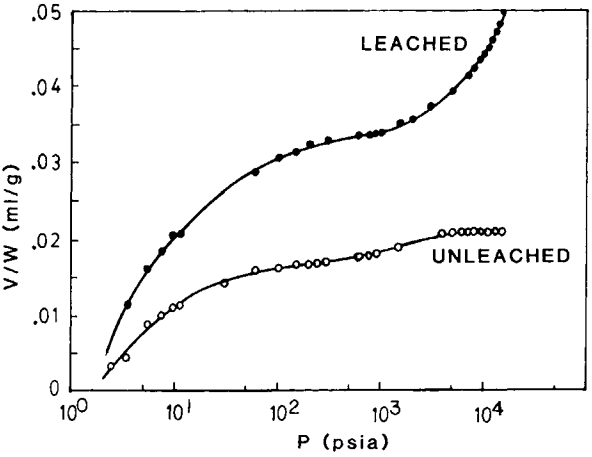

Fig. 13. Integral porosity–pressure curves of nylon 6 (O) containing 10.2 phr NaCl, (●) after leaching 10.2 phr NaCl.

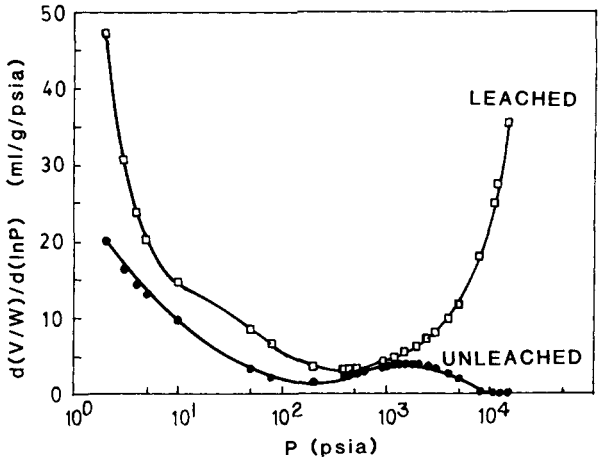

Fig. 14. Differential porosity curves derived from Fig. 13.

$D(\mu m)$ is a characteristic diameter and P (psia) is the pressure. Pore sizes of 100 μm are thus determined by P = 1.75 psia and 0.1–0.01 μm (1000–100 Å) by P = 1,750–17,500 psia. Roughly speaking, the 10^0–10^1 psia range detects pores having sizes similar to the dispersed salt particles while the 10^3–10^4 psia range detects tiny pores having sizes similar to crazes in glassy polymers.

Integral porosity–pressure curves are shown in Figure 11 for PS and SAN foams produced by complete removal of NaCl. The corresponding differential curves are shown in Figure 12. It is clearly seen that the distribution of pores is essentially bimodel; namely, coarse and very fine pores corresponding to sizes of leached out NaCl particles, crazes, and microcracks produced by the osmotic pressure. It is also seen that the volume fraction of the coarse pores constitutes only about one-third of the total porosity. This result is a reflection of the extensive deformation, fracturing, and crazing processes taking place during the leaching operation. Additionally, the total porosity results point out that open-cell structures are obtained by leaching only 5% v/v NaCl particles from

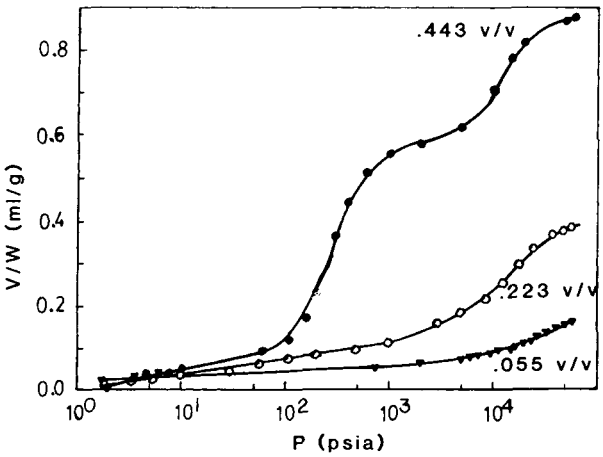

Fig. 15. Integral porosity–pressure curves of PMMA foams after leaching (▼) 0.055 v/v, (○) 0.223 v/v, (●) 0.443 v/v NaCl.

TABLE III
Comparison of Measured Porosities ϕ_p with Volume Fractions of Leached NaCl ϕ_s

Polymer	NaCl ϕ_s v/v fraction	Pores ϕ_p v/v fraction	"Extra Porosity"[a] $\phi_p - \phi_s$ v/v fraction
PMMA	0.055	0.16	0.105
PMMA	0.223	0.305	0.082
PMMA	0.443	0.51	0.067
PSF	0.207	0.387	0.18
PSF	0.322	0.48	0.158

[a] "Extra porosity" values reflect the porosity "added" during the leaching step by crazing and cracking, and the volume defects existing in the original polymer–halide granules.

PS and SAN, thus explaining the dramatic strength reduction in such "low porosity" foams.

Integral and differential porosity curves for nylon 6–NaCl particles and the corresponding nylon 6–void foams are shown in Figures 13 and 14. The total porosity in the nylon 6–NaCl particles is about 2% v/v with practically no tiny pores (10^3–10^4 psia range). The fraction of tiny pores in the nylon 6 foam is relatively small (in comparison with PS and SAN) because of its ductile behavior without crazing, and partial salt leaching by diffusion rather than by fracturing. In this regard, porosity–pressure curves for nylon 11 have a stronger resemblance to PS and SAN than those for nylon 6.

Integral porosity-pressure curves for PMMA foams are shown in Figure 15. The tiny pores are shown to constitute a major part of the porosity. Total porosity calculations show that the fractional porosities are always higher than the volume fraction of the NaCl that has been leached from the foams. A summary of these results and the resulting "extra porosity" are given in Table III. The extra porosity values for PMMA are about 8% v/v, while for the PSF foams they are about 17% v/v. PSF is thus interpreted as the polymer undergoing the most severe cracking and crazing processes during the NaCl leaching operation with water.

In summary, many parameters are playing roles in the leaching mechanism of salts from polymers with water. By careful systematic studies and understanding of the phenomena involved, however, one can select and control desired leaching rates and resulting foams structures. The scope of these studies can be extended to some failure cases of plastics in contact with water and to the surprising inertness found by the authors in some $CaCO_3$–polymer products in contact with strong acids.

References

1. D. J. Fossey and C. H. Smith, *J. Cell. Plast.*, **9**, 268 (1973).
2. R. S. Gregorian, U.S. Pat. 3,376,238 (1968).
3. D. M. Bigg, *Polym. Eng. Sci.*, **21**, 76 (1981).
4. T. L. Smith, *Trans. Soc. Rheol.*, **3**, 113 (1959).
5. C. R. Thomas, *Br. Plast.* **38**, 552 (1965).
6. L. E. Nielsen and B. Lee, *J. Comp. Mater.*, **6**, 136 (1972).
7. M. Narkis and E. Joseph, *J. Cell. Plast.*, **14**, 45 (1978).
8. M. Narkis and E. Joseph, *J. Appl. Polym. Sci.*, **22**, 3531 (1978).
9. M. Narkis, I. Berkovitz, L. Nicolais, and C. Migliaresi, *Polymer*, **19**, 1103 (1978).

10. L. Glas, "Polymeric Foams Produced by Extraction of Soluble Components," MSc Thesis, Technion, Haifa, 1981.
11. N. F. Cardarelli, *Controlled Release Pesticide Formulations*, CRC Press, Cleveland, Ohio, 1978.
12. N. Narkis and M. Narkis, *J. Appl. Polym. Sci.*, **20,** 3431 (1976).
13. E. Bianchi, A. Ciferri, A. Tealdi, R. Torre, and B. Valenti, *Macromolecules*, **7,** 495 (1974).
14. A. Siegmann and Z. Baraam, *J. Appl. Polym. Sci.*, **25,** 1137 (1980).
15. R. W. Lenz and R. S. Stein, Eds., *Structure and Properties of Polymer Films*, Plenum, New York, 1973, pp. 309–317.
16. P. Dunn and G. F. Sanson, *J. Appl. Polym. Sci.*, **13,** 1641 (1969); **13,** 1657 (1969).

Received September 23, 1981
Accepted November 19, 1981